Heating of refractory cathodes by high-pressure arc plasmas: I

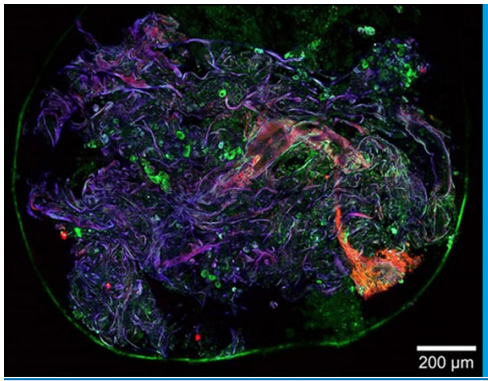

INSTITUTE OF PHYSICS PUBLISHING JOURNAL OF PHYSICS D: APPLIED PHYSICS

J. Phys. D: Appl. Phys. **35** (2002) 1736–1750 PII: S0022-3727(02)34419-X

Heating of refractory cathodes by high-pressure arc plasmas: I

M S Benilov and M D Cunha

Departamento de Física, Universidade da Madeira, Largo do Município, 9000 Funchal, Portugal

Received 1 March 2002, in final form 23 May 2002
Published 4 July 2002
Online at stacks.iop.org/JPhysD/35/1736

Abstract

A model of the near-cathode plasma layer in a plasma under a pressure of the order of one or several bars is reconsidered on the basis of recent theoretical results. Physics of the near-cathode layer is analysed in the range of near-cathode voltage drops of up to 50 V, in accord to recent experimental results which have shown that the near-cathode voltage drop in high-pressure arc discharges may be that high. It is found that a non-monotony of the dependence of the energy flux density on the surface temperature at fixed values of the near-cathode voltage drop is caused by one of the three mechanisms: overcoming of the increase of combined ion and plasma electron heating by the increase of thermionic cooling as the plasma approaches full ionization; non-monotony of the dependence of the ion current on the electron temperature which is caused by the deviation of the ion current from the diffusion value; rapid increase of the plasma electron heating which is subsequently overcome by thermionic cooling. A closed description of the plasma–cathode interaction is obtained by numerically solving the nonlinear boundary-value problem for the temperature distribution inside the cathode body. Results of numerical modelling of the diffuse discharge under conditions of a model arc lamp are given and a good agreement with the experimental data is shown.

1. Introduction

Advances achieved recently in the theory of current transfer to refractory cathodes of high-pressure arc discharges (see, e.g. review [1]) have been attained in the framework of a theoretical approach based on solving the equation of thermal conduction in the cathode body with a nonlinear boundary condition specifying the density of the energy flux from the plasma to the cathode surface as a function of (a local value of) the surface temperature and of the voltage drop across the near-cathode plasma layer. The latter function is obtained from a treatment of processes on the plasma side.

This approach was apparently first suggested in [2]. In addition to the mathematical formulation, in this work, in particular, a hypothesis was suggested that in general two or more solutions may exist for any given set of input conditions, corresponding to different modes of cathode operation. For a semi-infinite cathode, a model was treated which is based on dividing the surface into a cathode spot region of a certain radius in which the current (and heat) input is localized and a surrounding current-free region, and important considerations were given concerning this model. One-dimensional solutions describing the spotless, or diffuse, mode operation of rod-shaped cathodes have been obtained and found to correctly predict general trends in the variation of cathode temperature and heat transfer with cathode geometry and current, although a number of quantitative discrepancies occurred.

The above-described theoretical approach [2] has been known for about forty years and was apparently re-discovered, with some or other variations, more than once. Understanding of processes on the plasma side has considerably improved (see, for example, review [3]; some recent studies are cited in section 3). Unfortunately, advances in theoretical description of the plasma–cathode interaction on the whole (which includes answering the questions: How many modes exist under some or other particular conditions? What mechanisms govern each mode? How each mode can be self-consistently calculated?) for many years have been limited (see, e.g. reviews [3–5]). One should distinguish the work [6], in which an axially symmetric nonlinear thermal conduction problem

in a semi-infinite cathode was solved numerically without dividing the cathode surface into a current-collecting spot and a surrounding current-free region. Distributions of all parameters along the cathode surface have been determined without any additional considerations and found to describe a spot structure with a continuous transition from a current-collecting spot to a current-free periphery. Thus, it has been proved that the theoretical approach based on solving the nonlinear thermal conduction problem in the cathode body is capable of describing spot structures without dividing the cathode surface into a current-collecting spot and a surrounding current-free region. However, it had still remained unclear how (and, for that matter, *if*; see, for example, [7]) a model making use of existence of a current-collecting spot surrounded by a current-free region can be self-consistently derived. In fact, such-type theoretical models published until recently either have been incomplete (one parameter, usually the spot radius, remained indeterminate) and relied on empirical parameters, or employed arbitrary theoretical assumptions, such as some or other implementation of the 'principle' of minimum voltage.

Note that in [2] the voltage drop across the near-cathode layer was assumed to be constant along the cathode surface and was assumed to be control parameter of the problem, while in [6] the voltage drop on the near-cathode layer was assumed to be variable along the cathode surface and was determined from the current continuity equation in the expansion zone. Accordingly, the control parameter in [6] was the potential difference between the cathode surface and the bottom of the arc column. The voltage drop across the near-cathode layer determined in such a way depends on a distribution of conductivity of the near-cathode layer along the cathode surface. This means, in mathematical terms, that the dependence of the density of the energy flux from the plasma to the cathode surface on the surface temperature in the model [6] was non-local, i.e. the energy flux density was governed not only by the temperature of the considered point of the surface but also by temperatures of other points.

An approach similar to that of [6] was employed in the work [8], in which an axially symmetric nonlinear thermal conduction problem was solved numerically for a cylindrical cathode. A unique solution has been found for a cathode geometry modelling experimental conditions and two solutions have been found in a certain current range for a wide cathode (of a diameter equal to its height). The latter can be considered as an argument in favour of the above-mentioned hypothesis [2] on existence in the nonlinear thermal conduction problem in the cathode body of multiple solutions describing different modes. On the other hand, it remained obscure, e.g. why each of the two simultaneously existing solutions found in [8] just terminated rather than turned back or joined another solution, which would have been a behaviour typical of multiple solutions. Other interesting points which remained unclear were what is the general pattern of all the solutions existing and how important to existence of multiple solutions is the non-locality of the dependence of the density of the energy flux on the surface temperature, disregarded in [2] and taken into account in [6,8].

Advances in the theory of various modes of the plasma–cathode interaction in high-pressure arc discharges were achieved in the 1990s [9–18]. In [9–11], a self-consistent way to derive a closed model of current-collecting spot surrounded by a current-free region was found. A relationship governing the spot radius turned out to be represented by a condition of solvability of the problem describing the temperature distribution in a transition zone separating the spot and the current-free region. This result can be best understood in terms of the theory of nonlinear dissipative structures. From the point of view of this theory, the problem of contact of a current-collecting spot with a surrounding current-free region is a problem of coexistence of phases. Generally, the coexistence is possible only if a certain condition is satisfied (Maxwell's construction; see, for example, [19]). This condition results from a treatment of an intermediate (transition) region that separates the phases. In these terms, the above-mentioned solvability condition represents Maxwell's construction for the model considered, thus this model being an interesting example of a multidimensional problem in which Maxwell's construction can be formulated explicitly.

In [12], a thermal conduction problem with a local nonlinear boundary condition, governing the temperature distribution in the body of a model finite cathode, was treated by means of the bifurcation theory. It was proved that, under certain conditions, this problem has multiple multidimensional solutions for the same arc current, one of them describing the diffuse mode and others describing various spot modes. A general pattern of current–voltage characteristics corresponding to different modes found in [12] represents an interesting example of the bifurcation diagram of a bistable system.

Thus, the above-mentioned hypothesis [2] has been confirmed. One can conclude that the existence of multiple modes of current transfer to arc cathodes is not necessarily a manifestation of essentially different physical mechanisms, such as Schottky-amplified thermionic emission vs thermo-field or field emission. Rather, it may be described as a manifestation of non-uniqueness of multidimensional thermal balance of a finite body heated by an external energy flux depending in a nonlinear way on the local surface temperature.

Numerical modelling of multiple modes of steady-state current transfer to arc cathodes has been reported in [13–15]. In [16–18], spot-diffuse transitions on AC arc cathodes have been simulated.

As far as the plasma–cathode interaction in vacuum arcs is concerned (e.g. [1] and references therein), best developed at present are models based on considering this interaction as a collective phenomenon. (In other models, this interaction is treated as a sequence of individual events, termed microexplosions, or microspots, or fragments.) These models are not fundamentally different from the theoretical models of plasma–cathode interaction in high-pressure arcs. Therefore, the theoretical approach based on solving the nonlinear thermal conduction problem in the cathode body may be applied to describing plasma–cathode interaction also in vacuum arc discharges, its applicability being limited only by the assumption of a collective phenomenon.

Note that in the recent review on the theory of vacuum arcs [20], a closed collective-phenomenon model of a spot surrounded by a current-free region was considered, which has been obtained from analysis of processes on the plasma side (in a kinetic layer) as opposed to previous works, in particular

to [7, 21] in which the principle of minimum voltage was employed. It should be emphasized in this connection that, as is pointed out in [11], the difficulty in early models of a current-collecting spot surrounded by a current-free region originates in the loss of information which occurs when the condition of continuity of the heat flux, which holds at every point of the cathode surface, is replaced by only one condition, namely by equation of integral heat balance. Obviously, this difficulty cannot be satisfactorily overcome by invoking theoretical considerations which are unrelated to thermal conduction in the cathode. Having said this, one should conclude that the considerations cited in [20] are justified no better than the principle of minimum voltage.

This paper is a first part of a work concerned with a detailed study of various aspects of the interaction of a high-pressure plasma with refractory cathodes. The model of the near-cathode plasma layer [22] is reconsidered with account of recent theoretical results. Physics of the near-cathode layer is analysed in a wide range of near-cathode voltage drops, in accord to recent experimental results which have shown that the near-cathode voltage drop in high-pressure arc discharges may be much higher than most of the workers previously believed. Mechanisms are identified which cause non-monotony of the dependence of the energy flux density on the surface temperature at fixed values of the near-cathode voltage drop. Results of numerical solution of the equation of thermal conduction are given for the diffuse discharge under conditions of a low-current arc lamp, for which detailed electrical and thermal measurements have been performed recently [23–28]. A detailed comparison between theoretical and experimental results is performed and a good agreement is found. Results of numerical modelling of the diffuse mode at high currents and of spot modes will be reported in the second part of the work.

2. The model

The model employed in this work is essentially the same that was introduced in [2] (except the solution on the plasma side). We consider a thermionic cathode of a DC high-pressure arc discharge (see figure 1). A part of the cathode surface is in contact with the arc plasma and collects current from and is heated by the arc. Another part is in contact with the cold gas and may exchange heat with the gas and/or lose energy by means of radiation. The other part of the cathode surface is maintained at a fixed temperature T_c by external cooling. Thermal conductivity κ of the cathode material is assumed to be a known function of its temperature: $\kappa = \kappa(T)$. Joule heat generation inside the cathode body is negligible. It should be emphasized that the separation of the part of the cathode surface which is in contact with the arc plasma, from the part which contacts the cold gas, is introduced only for clarity of presentation and is not used while actually solving the problem.

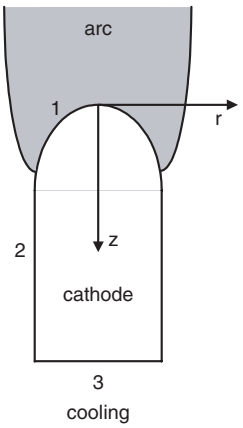

Figure 1. Schematic of the model: (1) current-collecting part of the cathode surface, (2) part of the cathode surface which is in contact with the cold gas, (3) part of the cathode surface which is externally cooled by a fluid.

The energy flux coming from the arc plasma to the current-collecting part of the cathode surface is generated in a thin near-cathode plasma layer. Current transfer across the layer is locally one dimensional and governed by a local value of the surface temperature T_w and by the voltage drop across the layer U. In such a situation, all parameters of the near-cathode plasma layer (in particular, densities of the energy flux and of the electric current from the plasma to the cathode surface) may be considered as functions of T_w and U. The voltage drop across the near-cathode layer, U, is assumed to be the same at all points of the current-collecting part of the surface. The heat exchange of the cathode with the cold gas and/or the radiation losses from the part of the surface which is in contact with the cold gas are assumed to be governed by a local value of the surface temperature T_w.

In such a situation, one can introduce a function $q = q(T_w, U)$ which is defined for all $T_w \geqslant T_c$ and describes the density of the energy flux to the part of the cathode surface that is in contact with the arc plasma and with the cold gas (i.e. to both parts 1 and 2 of the cathode surface indicated in figure 1). At high T_w, corresponding to the part of the surface which is in contact with the arc plasma, this function describes heating of the current-collecting surface by the plasma. At low T_w, corresponding to the part of the surface which is in contact with the cold gas, this function becomes independent of U and describes heat exchange of the cathode with the cold gas and/or radiation losses. In a similar way, one can introduce a function $j = j(T_w, U)$ which is defined for all $T_w \geqslant T_c$ and describes the density of electric current to the cathode surface. At high T_w, this function describes current transfer from the arc across the near-cathode plasma layer to the current-collecting part of the surface. At low T_w, this function vanishes.

If function $q(T_w, U)$ is known, the temperature distribution inside the cathode body and at the surface may be found by means of solving the equation of thermal conduction in the cathode body,

$$\nabla \cdot (\kappa \nabla T) = 0, \tag{1}$$

with the boundary condition

$$\kappa \frac{\partial T}{\partial n} = q(T_w, U) \tag{2}$$

at the part of the cathode surface which is in contact with the arc plasma and with the cold gas (here n is a direction locally orthogonal to the cathode surface and directed outside the cathode) and with the boundary condition

$$T = T_c \tag{3}$$

at the part of the cathode surface which is externally cooled.

After the problem (1)–(3) has been solved, one will know the temperature distribution over the cathode surface and will be able to calculate, using the (known) dependence $j = j(T_w, U)$, a distribution of the current density over the surface. Integrating the latter, one will find the arc current corresponding to a value of U being considered.

It should be emphasized that the near-cathode voltage drop U is considered in the problem (1)–(3) as a control parameter. This parameter should be chosen in such a way that the integral current to the cathode surface (i.e. the arc current) takes a prescribed value.

It should also be emphasized that what is specified in the framework of such an approach is not a distribution of the energy flux from the plasma over the cathode surface but rather a dependence of the energy flux density on the local surface temperature, this temperature being unknown *a priori*. In particular, no assumption is made as to what part of the cathode surface is current collecting and what part is in contact with the cold gas (in other words, boundary condition (2) equally applies to both parts 1 and 2 of the cathode surface indicated in figure 1). On having solved the thermal-conduction problem (1)–(3), one will have complete information on a temperature distribution in the cathode and also on a distribution of the energy flux and electric current over the cathode surface.

In the framework of the above approach, a description of the arc–cathode interaction may be constructed in three steps. At the first step, a (one dimensional) problem describing the current transfer across the near-cathode plasma layer is solved and all parameters of the layer are determined as functions of T_w and U. In particular, densities of the energy flux and of the electric current from the plasma to the current-collecting part of the cathode surface, $q_p = q_p(T_w, U)$ and $j = j(T_w, U)$, are determined.

The functions q_p and j determined at the first step are defined only for T_w high enough. At the second step, a function $q = q(T_w, U)$ must be introduced which is defined for all $T_w \geqslant T_c$, is close to q_p at high T_w, and describes at low T_w heat exchange of the cathode with the cold gas and/or radiation losses from the part of the surface which is in contact with the cold gas. The function j at low T_w may be set equal to zero. At the third step, the problem (1)–(3) is solved.

3. Solution on the plasma side

The aim of this section is to deal with the first step of the above-described procedure. In this work, the near-cathode plasma layer is calculated by means of a model similar to the model [22]. The latter model was developed for a plasma in the range of pressures of the order of 1 atm and has been used in a wide range of environments for both analytical treatment and numerical modelling [12, 22, 29–31]. In this work, modifications are introduced into the model [22] on the basis of results of recent studies. Calculation results are given and analysed in a wide range of near-cathode voltage drops, in accord to recent measurements which have shown that the near-cathode voltage drop in high-pressure arc discharges may reach values as high as 55 V [24].

Note that an alternative model of the near-cathode plasma can be found in [32]. This model has been used also by other workers [15, 33–35]. One should note that this model can hardly be considered as fully physically justified since it is based on a kinetics of ionization and recombination which does not conform to the principle of detailed balancing. Besides, it is unclear whether this model is capable of predicting high near-cathode voltages, observed in the experiment.

3.1. A model of the near-cathode layer

The near-cathode plasma layer (i.e. a region in which the energy flux to the current-collecting surface is formed) is assumed in the model [22], as well as in the most of preceding models, to be comprised by the space-charge sheath, which is adjacent to the cathode surface, and by the ionization layer, which is adjacent to the sheath. The surface is heated by ions produced in the ionization layer and accelerated by electric field in the space-charge sheath (which is assumed to be collision free for ions) and by fast plasma electrons which are capable of overcoming the potential barrier and of reaching the cathode surface. A dominating mechanism of cooling of current-collecting part of the cathode surface is cooling by thermionic emission.

One of the modifications introduced in this work into the model [22] was as follows. In the framework of this model, the density of the energy flux to the cathode surface generated by the plasma, q_p, is given by the following expression (equation (13) of [22]):

$$q_p = q_i + q_e - q_{em}, \tag{4}$$

where

$$q_i = J_i \left[ZeU_D + E - ZA_{eff} + k\left(2T_h + \frac{ZT_e}{2} - 2T_w\right)\right], \tag{5}$$

$$q_e = J_e(2kT_e + A_{eff}), \qquad q_{em} = J_{em}(2kT_w + A_{eff}). \tag{6}$$

Here and further q_i and q_e are the densities of energy fluxes delivered to the cathode surface by ions and by fast plasma electrons; q_{em} is the density of losses of energy by the cathode surface due to thermionic emission; J_i, J_e and J_{em} are the number densities of respective fluxes; $j_i = ZeJ_i$ is the density of the electric current delivered to the cathode surface by ions; $j_e = eJ_e$ is the density of electric current from the cathode to the plasma transported by fast plasma electrons; $j_{em} = eJ_{em}$ is the density of thermionic emission current; T_h and T_e are the temperatures of heavy particles (ions and neutral atoms) and of electrons in the near-cathode plasma layer; Z and E are the average charge number of ions and the average ionization energy in the near-cathode layer; U_D is the voltage drop in the space-charge sheath; A_{eff} is the effective (calculated with account of the Schottky correction) work function.

Designate by W_i work of the electric field over ions in the ionization layer. In the framework of the model [22], W_i is estimated as the average ion current in the ionization layer, $j_i/2$, times $U_i = U - U_D$ the voltage drop in the ionization layer (given by equation (16) of [22]). Equation (5) may be re-written as

$$q_i = J_i(ZeU_D + E - ZA_{eff}) + W_i + \left[J_i k\left(2T_h + \frac{ZT_e}{2}\right) - (J_i 2kT_w + W_i)\right]. \tag{7}$$

In the framework of the model [22], the first term in the square brackets on the right-hand side of equation (7) represents the flux of energy of ions leaving the ionization layer for the sheath. The second term represents sum of the flux of energy of neutral atoms that enter the ionization layer (with the same energy with which they have left the cathode surface after having been produced in neutralization of the coming ions) and of the work of the electric field over the ions in the ionization layer. In a steady state, these terms should be equal. (In fact, the condition of equality of these terms represents the equation of balance of the energy of heavy particles in the ionization layer.) Therefore, the last term on the right-hand side of equation (7) should be dropped and this equation assumes the form

$$q_{\mathrm{i}} = J_{\mathrm{i}}(ZeU_{\mathrm{D}} + E - ZA_{\mathrm{eff}}) + W_{\mathrm{i}}. \tag{8}$$

In this work, the ion energy flux density is determined by means of equation (8) instead of equation (5).

An equivalent form of equation (4) supplemented with equations (6) and (8) may be obtained as follows. The equation of balance of the electron energy in the ionization layer reads (equation (17) of [22]):

$$j_{\mathrm{e}}\left(2\frac{kT_{\mathrm{e}}}{e} + U_{\mathrm{D}}\right) + 3.2j\frac{kT_{\mathrm{e}}}{e} + J_{\mathrm{i}}E = j_{\mathrm{em}}\left(2\frac{kT_{\mathrm{w}}}{e} + U_{\mathrm{D}}\right) + W_{\mathrm{e}}. \tag{9}$$

Here $j = j_{\mathrm{i}} + j_{\mathrm{em}} - j_{\mathrm{e}}$ is the density of the net electric current from the plasma to the surface and W_{e} is work of the electric field over electrons in the ionization layer. Note that the terms on the left-hand side describe sinks of the electron energy in the ionization layer, namely, the flux of the energy carried away by fast electrons leaving the ionization layer for the sheath, the flux of the energy carried away by electrons leaving the ionization layer for the bulk plasma and the electron energy lost inside the layer for ionization. The terms on the right-hand side describe sources, namely, the energy brought in the layer by the emitted electrons accelerated in the space-charge sheath and the work of the electric field over the electrons inside the layer.

Substituting equations (6) and (8) into equation (4), adding the relationship obtained to equation (9) and making use of the formula $W_{\mathrm{e}} + W_{\mathrm{i}} = jU_{\mathrm{i}}$, one arrives at

$$q_{\mathrm{p}} = jU - \frac{j}{e}(A_{\mathrm{eff}} + 3.2kT_{\mathrm{e}}). \tag{10}$$

Equation (10) has a distinct physical sense: the plasma-related energy flux to the cathode surface represents the difference between the electrical power deposited per unit area of the near-cathode layer and the energy transported from the layer into the bulk plasma by a (electron) current, the latter being calculated with account of energy necessary for extracting electrons from the cathode. Obviously, the replacement of equation (5) by equation (8) amounts to using equation (10).

Another modification introduced in this work into the model [22] was as follows: in accord to the calculations [36] only simply charged ions were taken into account, a reason being that just these ions give a dominating contribution to the total ion current to the cathode surface. The third modification was that equation (41) of [37], which had been used in the model [22] to describe the dependence of the ion flux to the cathode surface on the ratio α of the ionization length to the mean free path for collisions of ions with neutral atoms, has been replaced in this work by equation (50) of [38].

Except the three above-described modifications, the model of this work coincides with the model [22]. The procedure of the solution is same that described in section 3.3 of [22].

Some results of calculations for the atmospheric-pressure argon plasma and a tungsten cathode are shown in figures 2–7. In the calculations, the parameter α was evaluated (according to equation (56) of [38]) in terms of the ionization rate constant, the latter being calculated as sum of the rate constant of direct ionization evaluated according to [39] and of the rate constant of stepwise ionization evaluated according to [38]. The cross section for collisions of the ions with neutral atoms was taken from [40]. Values of the work function and of the pre-exponential factor in the Richardson–Schottky formula were set equal to 4.55 eV and 6.02×10^5 A m^{-2} K^{-2}.

Note that one could think of supplementing the model with an equation of balance of the energy of heavy particles in the ionization layer, which is obtained by setting the last term on the right-hand side of equation (7) equal to zero. This equation, in principle, would allow one to determine self-consistently the heavy-particle temperature T_{h}. However, calculations for conditions of experimental interest have shown that a variation of T_{h} in a wide range does not produce an appreciable effect on results given by the above-described model (see section 5 below). Therefore, an equation of balance of the energy of heavy particles in the ionization layer was not used in this work and the heavy particle temperature was set equal to 4000 K.

3.2. Calculation results: particle fluxes from the plasma to the cathode surface

The density of the total (net) electric current from the plasma to the cathode surface along with its components, calculated for fixed U and variable T_{w}, is shown in figure 2. Also shown are the Schottky correction ΔA to the work function and the voltage drop in the ionization layer. Note that the data in this figure and the following ones are shown for values of the surface temperature which do not exceed a certain temperature above which q_{p} becomes negative, which would be a situation of no physical interest for reasons to be discussed in the next paper.

The current transported by fast plasma electrons represents a minor contribution in all the cases (it is smaller than the electron emission current). The current transported by ions represents a minor contribution in the whole range of T_{w} of interest in the case of low voltages (figure 2(*a*)). In the case of high voltages (figure 2(*b*)), the ion current exceeds the electron emission current at low T_{w} and is smaller than the electron emission current at high T_{w}. The electron emission current rapidly grows with increase of the surface temperature, which, of course, should have been expected, and so does the current of fast plasma electrons. The ion current rapidly grows at low T_{w}. At higher T_{w}, its growth slows down; in the case of high voltages (figure 2(*b*)), j_{i} passes through a maximum and then starts to decrease. The maximum value of j_{i} does not depend on U; for the atmospheric-pressure argon plasma this value equals 2.35×10^7 A^{-2} m^{-2}.

The Schottky correction to the work function increases with increase of the surface temperature in the case of low

voltages. In the case of high voltages, it increases at low T_w, then passes through a maximum and then decreases. The Schottky correction increases with increase of U at fixed T_w, except in the range of high U at high T_w where it weakly decreases (e.g. values of the Schottky correction corresponding to U equal to 10, 25, and 50 V are 0.13, 0.29, and 0.43 eV at $T_w = 3500$ K, while respective values at $T_w = 4300$ K are 0.23, 0.35, and 0.34 eV). The biggest value of the Schottky correction encountered in the present calculations is the one which corresponds to the point of maximum of the dependence of ΔA on T_w at $U = 50$ V and equals 0.45 eV. The respective value of the electric field strength at the cathode surface is 1.4×10^8 V m^{-1}. This electric field is within the thermionic emission domain [41]. Therefore, the electron emission current was determined by means of the Richardson–Schottky equation in all the calculations presented in this work.

The voltage drop in the ionization layer weakly decreases with increase of T_w in the case $U = 10$ V (figure 2(*a*)) and is about 0.5 of the total voltage drop in the near-cathode layer. In the case $U = 50$ V (figure 2(*b*)), U_i weakly decreases at low surface temperatures, then passes through a minimum and then increases, reaching values of the order of 0.3 of the total voltage drop. Note that absolute values of U_i in the case $U = 50$ V may be rather high (above 10 V).

The non-monotonic nature of the dependence of the ion current density on the surface temperature shown in figure 2(*b*) may be understood as follows. The ion current density is governed in the present model by the electron and heavy-particle temperatures and by the plasma pressure. The dependence on the electron temperature for atmospheric-pressure argon at $T_h = 4000$ K is shown in figure 3. Dotted lines in this figure represent the parameter α and the (equilibrium) ionization degree ω at the edge of the ionization layer. The dashed line represents the ion current density evaluated in the diffusion approximation, which has been found by means of the formula [42]

$$J_i = \left(1 + \frac{T_e}{T_h}\right) \frac{D_{ia} n_{i\infty}}{d}, \tag{11}$$

where D_{ia} is the coefficient of binary diffusion ion-atom, $n_{i\infty}$ is the (equilibrium) number density of the ions at the edge of the ionization layer and d is the ionization length.

At low values of the electron temperature, when the ionization degree is much smaller than unity, the ionization length is approximately inversely proportional to $n_{i\infty}$. Since $n_{i\infty}$ in a weakly ionized plasma rapidly increases with increase of T_e, the ion current density at low T_e, being proportional to $n_{i\infty}^2$, grows very rapidly. As the electron temperature increases and the ionization degree becomes comparable to unity, the increase of $n_{i\infty}$ slows down and so does the increase of the ion current. As the electron temperature increases further and the plasma approaches full ionization and then becomes fully ionized, $n_{i\infty}$ starts decreasing. However, the product $(1 + T_e/T_h)n_{i\infty}$ in a fully ionized plasma is constant (it coincides, to the accuracy of a factor, with the plasma pressure). Hence, the ion current density in a fully ionized plasma evaluated in the diffusion approximation is inversely proportional to the ionization length. The latter

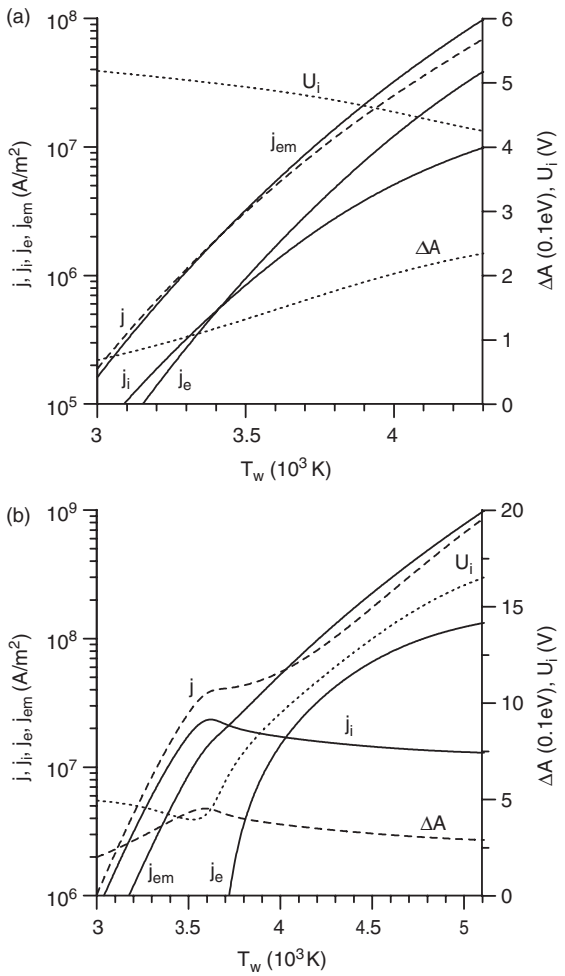

Figure 2. Density of the electric current from the plasma to the cathode surface and its components vs the surface temperature. (*a*) $U = 10$ V, (*b*) $U = 50$ V.

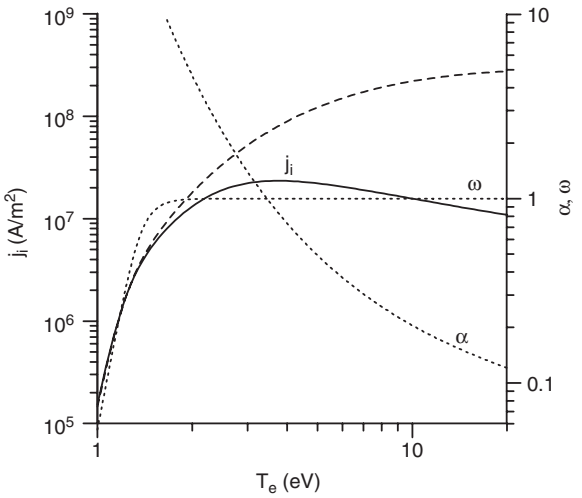

Figure 3. Ion current density to the cathode surface, parameter α characterizing ratio of the ionization length to the mean free path for collisions of an ion with neutral atoms, and the ionization degree at the edge of the ionization layer vs the electron temperature. Dashed line: the ion current density evaluated in the diffusion approximation.

is approximately proportional to $\sqrt{T_e/k_i}$ for a fully ionized plasma, where k_i is the ionization rate constant. In the electron temperature range considered, k_i increases with increase of T_e faster than T_e. Hence, the ionization length decreases and the ion current density increases at high T_e, although much slower than at low T_e.

Thus, the ion current evaluated in the diffusion approximation increases in the whole range of T_e considered, and this is what can be seen in figure 3. However, the diffusion theory provides a good approximation only at low T_e, when the mean free path for collisions of ions with neutral atoms is much smaller than the local length scale (represented by the ionization length), i.e. when $\alpha \gg 1$. As T_e grows and α becomes comparable to and then much smaller than unity, the growth of the ion current becomes slower than that predicted by the diffusion theory and then gives way to a decrease. The maximum value of the ion current density depicted in figure 3 equals $2.35 \times 10^7\,\mathrm{A\,m^{-2}}$ (which is the same as the maximum value of the dependence of j_i on T_w shown in figure 2(b)) and is attained at $T_e \approx 3.7\,\mathrm{eV}$. It should be emphasized that the latter value is considerably higher than those at which the plasma becomes fully ionized; in other words, there is no direct relation between the limitation of the ion current and the full ionization of the plasma.

Now the monotony of the dependence of j_i on T_w shown in figure 2(a) and the non-monotony of the one in figure 2(b) can be understood if the electron temperature in the near-cathode layer does not reach the above-mentioned value of 3.7 eV under conditions of figure 2(a) and exceeds this value under conditions of figure 2(b). This is indeed the case, which can be seen from figure 4 where the electron temperature is shown for the same conditions as those of figure 2. Also shown in this figure are quantities r_E, r_e, r_j, r_i which are defined as the ratios of, respectively, the second term on the right-hand side, the first, second and third terms on the left-hand side of equation (9) to sum of the terms on the right-hand side. Thus, r_E represents a contribution of work of the electric field over electrons inside the ionization layer to the total input of the electron energy while r_e, r_j, and r_i represent contributions of different sinks of the electron energy in the ionization layer.

The contribution of work of the electric field in all the cases does not change much with the surface temperature. Hence, the total input of the electron energy in the ionization layer increases, with increase of T_w, approximately proportionally to j_{em}. At low surface temperatures, the major sink of the electron energy is through losses for ionization; the ion current density grows with increase of T_w approximately proportionally to j_{em}. As discussed above, the ion current density increases with increase of the electron temperature very rapidly at low ω; therefore, the electron temperature increases in the range of low T_w relatively slowly.

As the surface (and electron) temperature increases, the contribution of the ionization losses decreases and transport of energy by the electrons leaving for the bulk plasma becomes the major sink of the electron energy. The electron temperature starts growing faster.

As T_w grows further, the increase of the electron temperature in the case of high voltages slows down once again. One can see from figure 4(b) that this happens when another sink mechanism comes into play, namely, transport of energy by electrons leaving for the sheath.

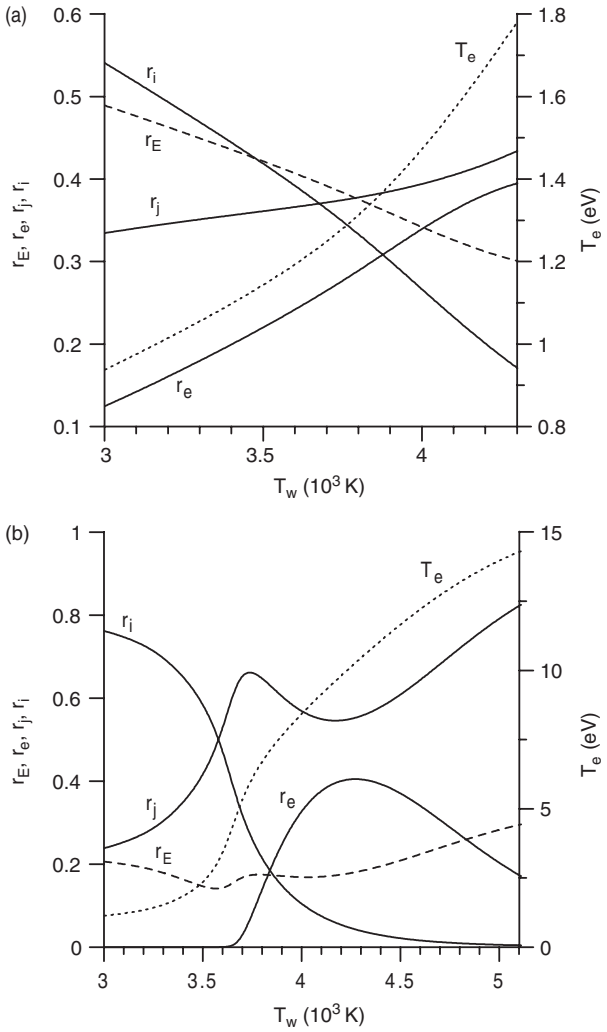

Figure 4. Parameters of the near-cathode plasma layer vs the cathode surface temperature. T_e: electron temperature in the near-cathode layer; r_E, r_e, r_j, r_i: contributions of different mechanisms governing balance of the electron energy in the ionization layer. (a) $U = 10\,\mathrm{V}$, (b) $U = 50\,\mathrm{V}$.

3.3. Calculation results: energy flux from the plasma to the cathode surface

The density of the energy flux to the cathode surface generated by the plasma, calculated for fixed U and variable T_w, is depicted in figure 5. Dashed lines represent data obtained without the first and third modifications introduced in this work into the model [22], i.e. obtained with the use of equation (5) rather than equation (8) and of equation (41) of [37] rather than equation (50) of [38]. One can see that the dashed lines are not distant from the solid ones, i.e. the effect produced by these modifications is not considerable. Also shown are results of calculations performed by means of the model of this work without the second modification, i.e. by means of the model of this work with account of doubly and triply charged ions on the basis of assumption of ionization equilibrium as described in [22]. One can see that the effect of absence of multiply charged ions is minor at $U \lesssim 12\,\mathrm{V}$, when the electron temperature is low and the density of multiply charged ions is negligible anyway [22]. At higher U, this effect is inessential

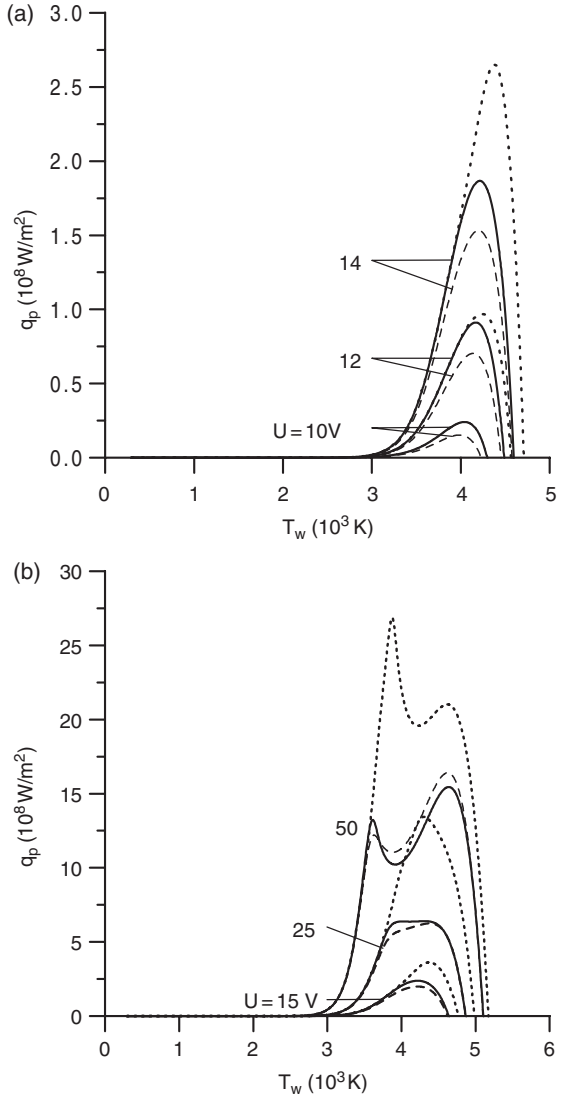

Figure 5. Density of the energy flux from the plasma to the cathode surface vs the surface temperature. Solid lines: calculation by means of the model of this work. Dashed lines: calculation by means of the model of this work without the first and third modifications. Dotted lines: calculation by means of the model of this work without the second modification.

at moderate T_w corresponding to the growing section of the function q; at higher T_w this effect comes into play and results in a decrease of the energy flux by a factor of up to approximately 2.

In the range $U \lesssim 20$ V, the dependence of q_p on T_w for fixed U includes a growing and falling sections separated by a maximum and is similar to that calculated for this range in [22]. (In fact, similar graphs can be found already in the work [2], except that those graphs are not smooth at the maximum point.) At higher U, the dependence changes: a plateau appears, which subsequently gives way to two maxima and a minimum. With increase of U at fixed T_w, the energy flux density increases very rapidly at low U and considerably slower at higher U.

The reason of such a behaviour of the function q_p is illustrated in figure 6, where the components of the energy flux are shown. The density of the net plasma-related energy flux, the electron temperature and the ionization degree at the edge of the ionization layer are also shown for convenience. In the case $U = 10$ V (figure 6(a)), balance between heating and cooling is rather delicate: the net energy flux is much smaller than either heating or cooling in the whole range of surface temperatures of interest. At low and moderate T_w, the

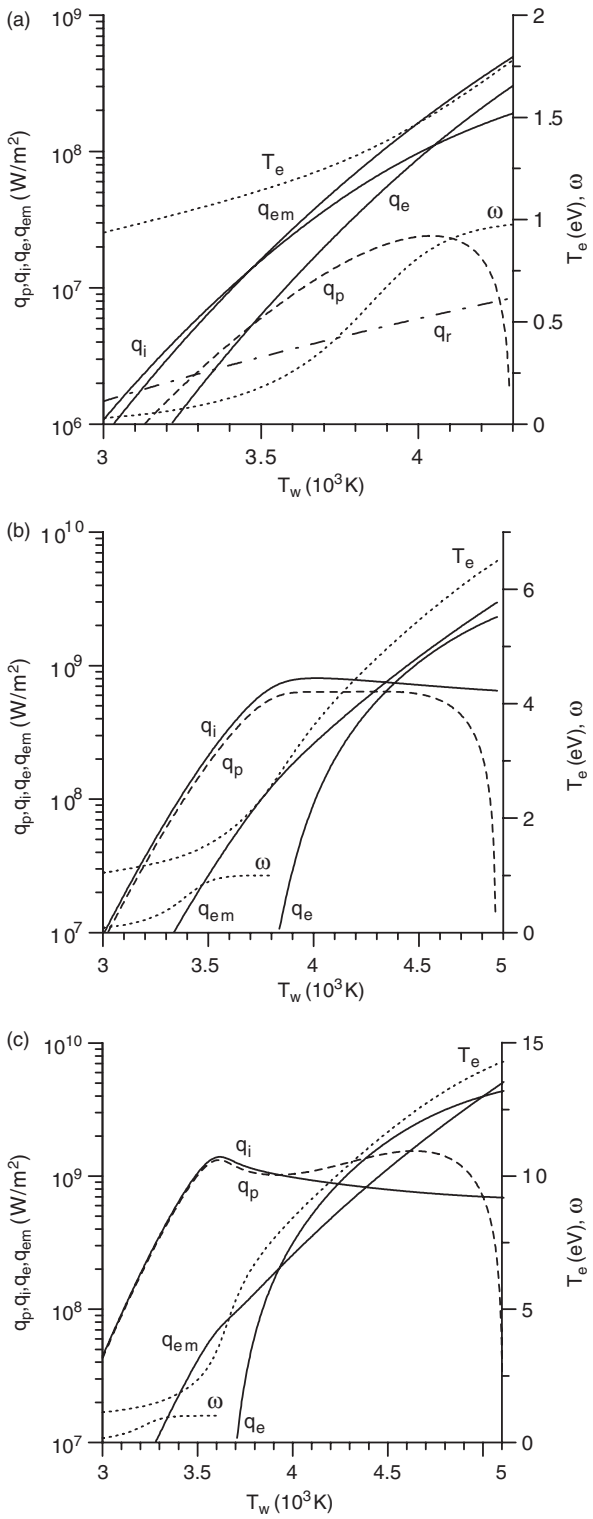

Figure 6. Components of the energy flux from the plasma to the cathode surface vs the surface temperature. (a) $U = 10$ V (also shown are the radiation losses), (b) $U = 25$ V, (c) $U = 50$ V.

ion heating exceeds substantially the heating by fast plasma electrons; however, the latter cannot be discarded since it is comparable to or exceeds the net energy flux.

At low T_w, all components of the energy flux grow with increase of T_w approximately proportionally to j_{em}; combined ion and plasma electron heating grows faster than thermionic cooling and the net energy flux to the cathode surface increases. As T_w increases and the ionization degree approaches unity, the increase of the ion current slows down; the increase of thermionic cooling overcomes increase of combined ion and plasma electron heating and the net energy flux starts to decrease. Another interpretation is suggested by equation (10): the electron temperature increases in the range of low T_w relatively slowly; the quantity $U - (A_{eff} + 3.2kT_e)/e$ does not change much and q_p increases approximately proportionally to j. As T_w increases, the rate of increase of the electron temperature grows; eventually the second term on the right-hand side of equation (10) starts to grow faster than the first term and the dependence of q_p on T_w starts falling.

It should be emphasized that the parameter α is large at $U = 10\,\mathrm{V}$ in the whole range of T_w considered (exceeds 7). Hence, the non-monotony of the dependence of q_p on T_w at low voltages may be understood in the framework of the diffusion approximation and is caused by the above-discussed slowing down of the increase of the ion current which occurs when the plasma becomes strongly and then fully ionized.

In the cases $U = 25\,\mathrm{V}$ and $U = 50\,\mathrm{V}$ (figures 6(*b*) and (*c*)), at low and moderate T_w the ion heating exceeds substantially both thermionic cooling and plasma electron heating, so the net energy flux density is governed solely by the ion heating. In the case $U = 25\,\mathrm{V}$, the ion heating gets nearly saturated at moderate T_w, and so is the net energy flux. As T_w grows further, thermionic cooling and plasma electron heating come into play. However, the respective energy fluxes are nearly compensated, and since the ion heating remains close to saturation, the net energy flux also remains nearly constant. At $T_w \gtrsim 4500\,\mathrm{K}$, the increase of thermionic cooling finally overcomes the increase of plasma electron heating and the net energy flux starts falling.

Physics in the case $U = 50\,\mathrm{V}$ is similar except that the net energy flux at moderate T_w first decreases, which is due to a decrease of the ion heating, and then increases, which is due to a rapid increase of the plasma electron heating. This is an explanation of the two maximum points of the dependence of q_p on T_w at high-voltage drops, which can be seen in figure 5(*b*). It should be emphasized that the first maximum point originates in the above-discussed deviation of the ion flux to the cathode surface from the diffusion value and therefore cannot be understood in the framework of the diffusion approximation, in contrast to the maximum point at low voltages. While the maximum at low voltages occurs as the plasma approaches full ionization, the first maximum at high voltages occurs when the plasma is already fully ionized, in agreement to the discussion of figure 3. This can be distinctly seen from figure 6(*a*), on the one hand, and from figure 6(*c*), on the other.

The dependence of the energy flux density on U at fixed T_w is illustrated in figure 7. One can see that the rapid increase of q_p at low U is a consequence of a rapid increase of the ion heating, which, in turn, results from a rapid increase of the ion current. Note that the ionization degree under the conditions of figure 7 exceeds 50% even at low U, while α at low U is much larger than unity. Hence, the rapid increase of the ion current at low U is due mainly to a rapid decrease of the ionization length.

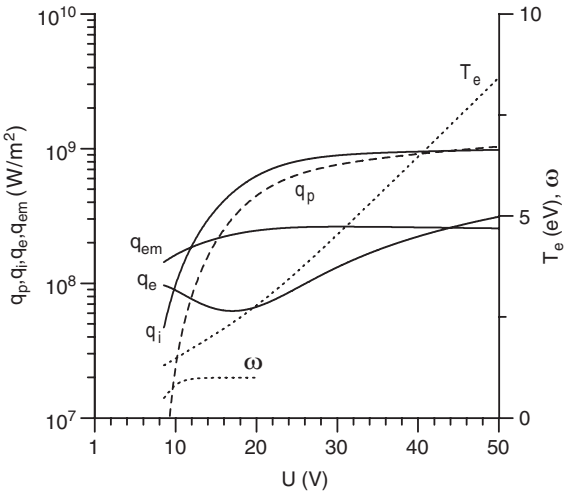

Figure 7. Density of the energy flux from the plasma to the cathode surface vs the near-cathode voltage drop. $T_w = 4000\,\mathrm{K}$.

4. Energy losses from the part of the cathode surface which contacts the cold gas

At the second step of the procedure described in section 2, function q_p should be extended down to $T_w = T_c$ in such a way as to describe the energy flux from the part of the surface which is in contact with the cold gas. In this work, the latter energy flux is assumed to be dominated by radiation losses.

We calculate the radiation losses q_r by means of the formula $q_r = \varepsilon\sigma T_w^4$, where ε is the emissivity evaluated in accord to [43] and σ is the Stefan–Boltzmann constant. The losses determined in such a way are shown in figure 6(*a*). One can see that the losses are not substantial at the current-collecting part of the cathode surface. However, calculations for experimental conditions to be considered below show that radiation losses from the lateral surface of the cathode, which is in contact with the cold gas, are quite substantial, especially if the cathode is tall.

Function q which describes the density of the energy flux to the part of the cathode surface that is in contact with the arc plasma and with the cold gas (i.e. to both parts 1 and 2 of the cathode surface indicated in figure 1) may be obtained by subtracting q_r from the density of the plasma-related energy flux, q_p:

$$q = q_p - q_r. \tag{12}$$

Note that equation (12) cannot be used at T_w below a certain temperature, since difficulties arise in solving equations for the near-cathode plasma layer under conditions at which there is practically no plasma adjacent to the cathode. Therefore, equation (12) has been used in calculations for tungsten cathodes at $T_w \geqslant 2000\,\mathrm{K}$; at $T_w < 2000\,\mathrm{K}$, q was set equal to $-q_r$. Since q_p at $T_w = 2000\,\mathrm{K}$ varies between $47\,\mathrm{W\,m^{-2}}$ at $U = 10\,\mathrm{V}$ and $1.7 \times 10^3\,\mathrm{W\,m^{-2}}$ at

$U = 50$ V while the radiation losses at this temperature equal 2.1×10^5 W m^{-2}, a discontinuity of the dependence of q on T_w, determined in such a way, at the point $T_w = 2000$ K is negligible. It should be emphasized that the exclusion of the first term on the right-hand side of equation (12) at $T_w < 2000$ K has purely a technical sense and the temperature $T_w = 2000$ K should not be identified with the temperature of the cathode surface at the border between regions 1 and 2 in figure 1.

The function j is evaluated by means of the approach described in section 3 at $T_w \geqslant 2000$ K and is set equal to zero at $T_w < 2000$ K. Note that the current density, evaluated at $T_w = 2000$ K by means of the approach described in section 3, does not exceed 4×10^{-5} A mm^{-2}. The lateral surface of cathodes in the experimental conditions to be considered below does not exceed 140 mm^{-2}. Hence, the error caused by neglecting the current density in the range $T_w < 2000$ K does not exceed 6 mA, which is well below the accuracy of the experiment.

Substituting equation (10) into equation (12) and integrating the relationship obtained over the part of the cathode surface that is in contact with the arc plasma and with the cold gas, one gets

$$IU = Q_c + Q_r + \frac{I}{e}(A^*_{eff} + 3.2kT^*_e), \tag{13}$$

where

$$Q_c = \int q \, dS, \qquad Q_r = \int q_r \, dS,$$
$$A^*_{eff} = \frac{1}{I}\int j A_{eff} \, dS, \qquad T^*_e = \frac{1}{I}\int j T_e \, dS, \tag{14}$$

the integrals being extended over the part of the cathode surface that is in contact with the arc plasma and with the cold gas. Note that Q_c is the total power removed by thermal conduction from the surface inside the cathode body and then to the cooling fluid, Q_r is the total power irradiated from the cathode surface, A^*_{eff} and T^*_e are weighted average values of the effective work function and of the electron temperature. Physical sense of equation (13) is quite clear: the electrical power deposited in the near-cathode layer, IU, equals sum of the power transported from the layer to the cathode and then from the cathode to its environment, $Q_c + Q_r$, and of the power transported from the layer into the bulk plasma by the (electron) current, $I(A^*_{eff} + 3.2kT^*_e)/e$.

5. Modelling the diffuse mode in a low-current arc

In this work, the nonlinear boundary-value problem (1)–(3) with function $q(T_w, U)$ described by equation (12) is solved numerically for the case of axially symmetric temperature distributions. An iterative approach is used. On each iteration, the (linearized) problem is solved by means of a finite-difference numerical scheme. With respect to solving the grid equations, we have found that iterative methods such as successive overrelaxation are not robust enough. Therefore, the grid equations are solved by means of a variant of LU decomposition (e.g. [44]).

Input parameters for calculations are plasma-producing gas and its pressure, cathode geometry and material, and near-cathode voltage; all other parameters are found, including temperature distribution in the cathode body and on the surface, the current density distribution over the cathode surface, the arc current, the power removed by thermal conduction to the cooling fluid, and the power irradiated from the cathode surface. Solving the problem for different values of the near-cathode voltage drop, one can obtain a complete description of the current–voltage characteristic of the cathodic part of the discharge.

Calculations reported in this section refer to the diffuse discharge under conditions of low-current arc experiments [23–28]. Some additional modelling results for these conditions can be found in [28]. Results of numerical modelling of the diffuse mode at high currents and of spot modes will be reported in the second part of the work.

In figures 8–16, modelling results are shown for the argon plasma under the pressure of 2.6 atm and cylindrical cathodes made of tungsten or thoriated tungsten (R is the radius of a cathode and h is its height). Thermal conductivity of tungsten was taken from [45]. The cooling temperature T_c was set equal to the room temperature. Thermal conductivity and emissivity of thoriated tungsten were set equal to those of (pure) tungsten. Values of the work function and of the pre-exponential factor in the Richardson–Schottky formula used in calculations for thoriated tungsten (0.7% thorium) were 3.88 eV and 2.11×10^5 A m^{-2} K^{-2}; these values have been obtained by interpolation between the values for pure tungsten mentioned at the end of section 3.1 and the values of 2.63 eV and 3.0×10^4 A m^{-2} K^{-2} which are employed usually (e.g. [22, 46]) for thoriated tungsten with 2% thorium. (The interpolation of the work function and of logarithm of the pre-exponential factor was linear in thorium percentage.) In calculations for thoriated-tungsten cathodes, the first term on the right-hand side of equation (12) was excluded at $T_w < 1700$ K; note that q_p at $T_w = 1700$ K varies between 14 W m^{-2} at $U = 10$ V and 398 W m^{-2} at $U = 50$ V and is much smaller than the respective radiation losses which are equal to 0.98×10^5 W m^{-2}.

In figure 8, power removed by thermal conduction to the cooling fluid and power irradiated from the surface of a tungsten cathode are shown. According to both the theory and the experiment, radiation losses are more significant than thermal conduction losses. Obviously, this is a consequence of large values of the ratio h/R for the cathodes considered. An interesting result is that while radiation losses increase with increasing current, thermal conduction losses are nearly constant. As h decreases, thermal conduction losses increase while radiation losses decrease, as it could be expected. The agreement between the modelling and experiment is good, especially on thermal conduction losses.

The temperature at the centre of the front surface of the cathode slowly increases with increasing current (see figure 9). The temperature is nearly independent of the cathode length. As it could be expected, the surface temperature decreases with a decrease of the work function of the cathode material. Again, the agreement between the theory and experiment is good.

Current–voltage characteristics are shown in figure 10 for tungsten cathodes and in figure 11 for a cathode made

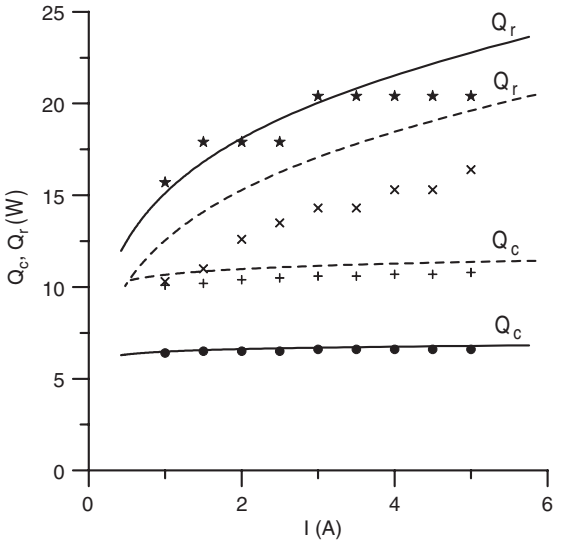

Figure 8. Power removed by thermal conduction to the cooling fluid and power irradiated from the surface of a tungsten cathode. $R = 0.5$ mm. Lines: modelling; points: experiment [24]. Q_c (•, +): power removed by thermal conduction. Q_r (⋆, ×): irradiated power. Solid lines (•, ⋆): $h = 30$ mm. Dashed lines (+, ×): $h = 20$ mm.

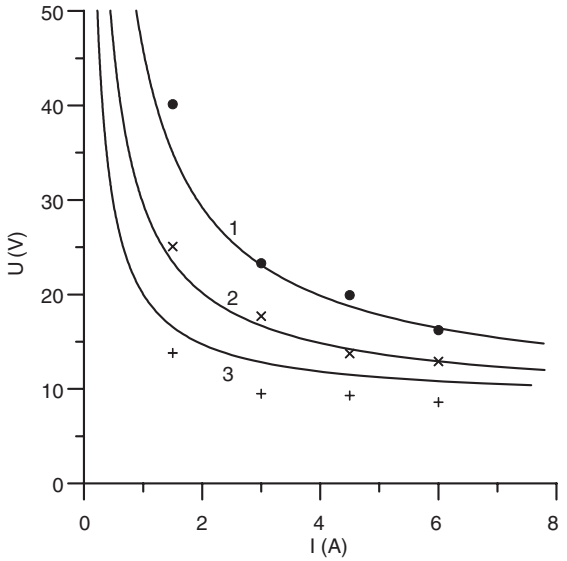

Figure 10. Current–voltage characteristics of tungsten cathodes. Lines: modelling. (•): experiment [23], (×, +): experiment [25]; 1 (•): $R = 0.75$ mm, $h = 24$ mm. 2 (×): $R = 0.5$ mm, $h = 25$ mm. 3 (+): $R = 0.3$ mm, $h = 15$ mm.

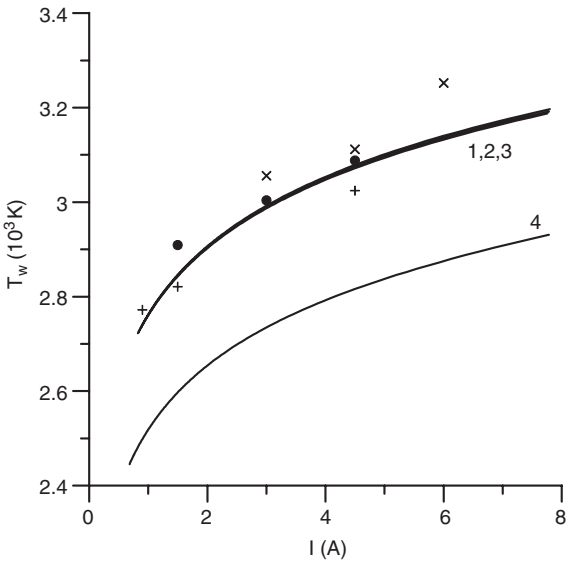

Figure 9. Temperature at the centre of the front surface of the cathode. $R = 0.75$ mm. Lines: modelling; points: experiment [47]. 1, 2, 3 (×, •, +): tungsten cathode. 4: thoriated-tungsten cathode. 1 (×): $h = 29$ mm. 2, 4 (•): $h = 24$ mm. 3 (+): $h = 19$ mm.

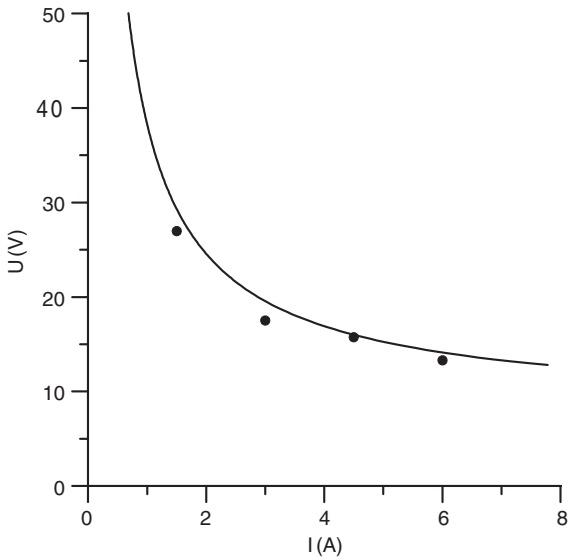

Figure 11. Current–voltage characteristics of a thoriated-tungsten cathode. Line: modelling; points: experiment [23]. $R = 0.75$ mm, $h = 24$ mm.

of thoriated tungsten. According to both the theory and the experiment, the current–voltage characteristics are falling in the current range considered. The voltage drop decreases with a decrease of the work function of the cathode material, as it should be expected. Again, the agreement between the theory and experiment is good.

The data shown in figures 9–11 have been obtained with the use of the assumption $T_h = 4000$ K, as well as all the other data given in this work. In order to check this assumption, two additional sets of calculations have been performed for the conditions of figures 9–11: one with $T_h = T_w$ and another with $T_h = 10^4$ K. Both sets produced results which coincided, with the graphical accuracy, with those obtained with $T_h = 4000$ K, in accord to what has been said at the end of section 3.1.

In figure 12, power transported from the near-cathode plasma layer to the cathode, $Q_c + Q_r$, is compared with the power input into the layer, IU (cf equation (13)). Also shown are experimental data on power transported to the cathode [24] (these data correspond to sum of quantities Q_c and Q_r shown in figure 8). Although U decreases with increase of I, the power input into the near-cathode layer increases. Power transported to the cathode also increases, which is consistent with the above-mentioned increase of the cathode temperature with increasing current.

One can see from figure 12 that at very low currents nearly all the power supplied to the near-cathode plasma layer is

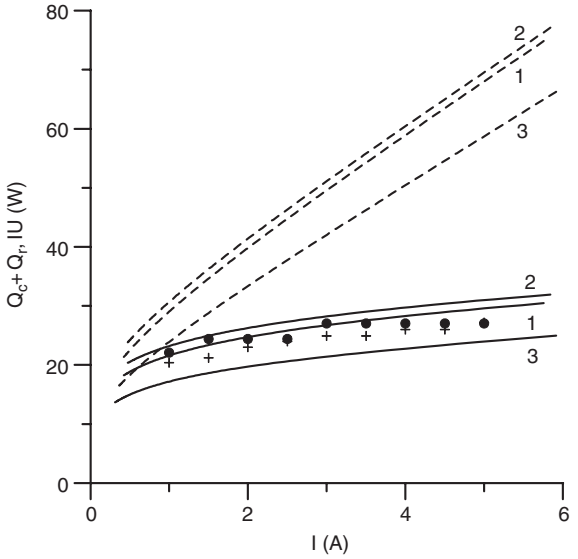

Figure 12. Power balance of the near-cathode plasma layer. Lines: modelling; points: experiment [24]. Solid, points: power transported to the cathode, $Q_c + Q_r$. Dashed: power input into the near-cathode layer, IU. $R = 0.5$ mm; 1, 2, points: tungsten cathode; 3: thoriated-tungsten cathode; 1, 3 (•): $h = 30$ mm; 2 (+): $h = 20$ mm.

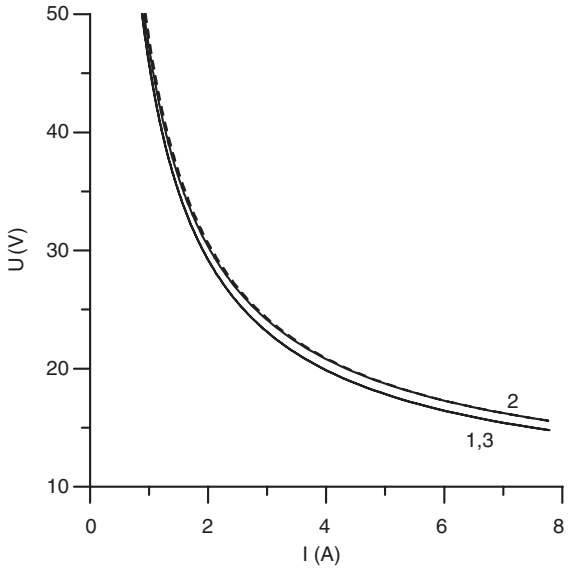

Figure 13. Current–voltage characteristics of a tungsten cathode. $R = 0.75$ mm, $h = 24$ mm. 1: Calculation by means of the model of this work; 2: calculation by means of the model of this work without the first modification; 3: calculation by means of the model of this work without the second and third modifications. Dashed: calculation by means of the model of this work neglecting current transfer to the lateral surface of the cathode.

transported to the cathode. With increase of current, fraction of power transported to the cathode decreases considerably, which means that fraction of power transported by electrons to the bulk plasma considerably increases. Having in mind that U decreases with increase of current, one should conclude that this result is related to another modelling result mentioned above in connection with discussion of figure 6(a): at low voltages, the net plasma-related energy flux to the cathode surface is much smaller than thermionic emission cooling. Note that the fact that fraction of power transported by electrons to the bulk plasma is variable and may be quite substantial obviously hinders determination of the near-cathode voltage drop from calorimetric measurements.

In figure 13 (solid) lines 1–3 illustrate an effect produced on the calculation results by modifications introduced in this work into the model of the near-cathode layer [22] (see section 3.1). One can see that the only modification that produces a visible effect under these conditions is the first one, i.e. the replacement of equation (5) by equation (8). However, even this effect is small. Obviously, this contributes to credibility of the modelling for the conditions considered.

Also shown in figure 13 are results of modelling performed for the case when the lateral surface of the cathode is electrically insulating. (In these calculations, the energy flux density at the lateral surface was set equal to $-q_r$ and the electric current density at the lateral surface was set equal to zero.) One can see that the current–voltage characteristics of the variants with and without current collection by the lateral surface are quite close. However, the current distributions along the cathode surface are essentially different: in the case with current collection by the lateral surface, the current collected by this surface at I equal to, for example, 4 A is 2.9 A.

Note that the integral power balances of the cathode for these two variants are also very close: the total power losses $Q_c + Q_r$ at $I = 4$ A are 49.2 W with current to the lateral surface and 51.9 W without. Furthermore, distributions of losses between thermal conduction and radiation losses are also quite similar: Q_c and Q_r at $I = 4$ A are, respectively, 20.7 and 28.5 W with current to the lateral surface and 20.8 and 31.1 W without. However, this power is supplied by the plasma in essentially different ways: in the variant with current to the lateral surface, the power supplied through the lateral surface (which is obtained by integrating q_p over the lateral surface) is 35.5 W.

One can conclude that integral characteristics of the cathode are not strongly affected by a distribution of current and power over the top of the cathode under the conditions considered.

Distributions of parameters along the cathode surface are illustrated by figures 14–16. Here, r and z are cylindrical coordinates with the origin at the centre of the front surface of the cathode and with the z-axis directed from the front surface into the cathode body. (These coordinates are illustrated by figure 1 with the difference that top of the cathode is flat in the present modelling rather than half-spherical as shown in figure 1.) In accord with this choice, $\{r \leqslant R, z = 0\}$ is the (circular) front surface of the cathode while $\{r = R, z \geqslant 0\}$ is the (cylindrical) lateral surface, so the range $0 \leqslant r + z \leqslant R$ in figures 14–16 corresponds to the front surface while the range $r + z \geqslant R$ corresponds to the lateral surface.

One can see from figure 14 that the temperature distribution along the cathode surface is non-monotonic. As it could be expected, the hottest point of the cathode is the edge of the front surface, where conditions for thermal-conduction heat removal are the worst. The variation of the temperature along the front surface of the cathode is very small, which is again a consequence of small values of the ratio R/h for the cathodes

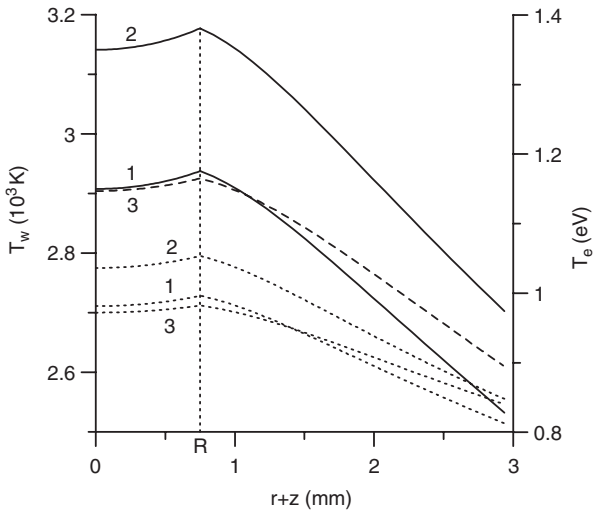

Figure 14. Distributions of the cathode surface temperature and of the electron temperature in the near-cathode layer along the surface of a tungsten cathode. Solid, dashed: surface temperature; dotted curves: electron temperature. $R = 0.75$ mm. 1: $I = 2$ A, $h = 19$ mm; 2: $I = 6$ A, $h = 19$ mm; 3: $I = 2$ A, $h = 29$ mm.

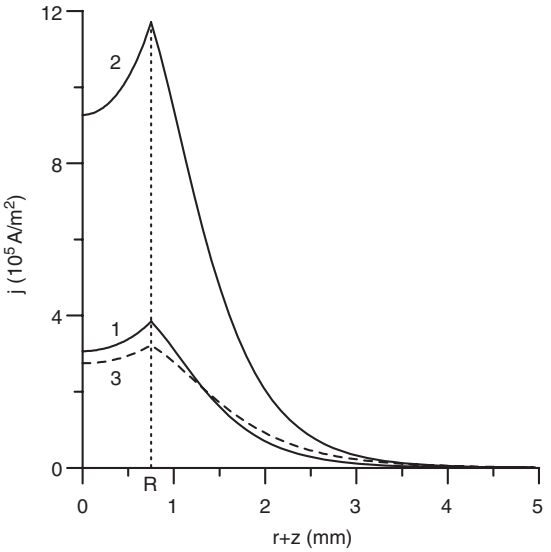

Figure 15. Distribution of the current density along the surface of a tungsten cathode. $R = 0.75$ mm. 1: $I = 2$ A, $h = 19$ mm; 2: $I = 6$ A, $h = 19$ mm; 3: $I = 2$ A, $h = 29$ mm.

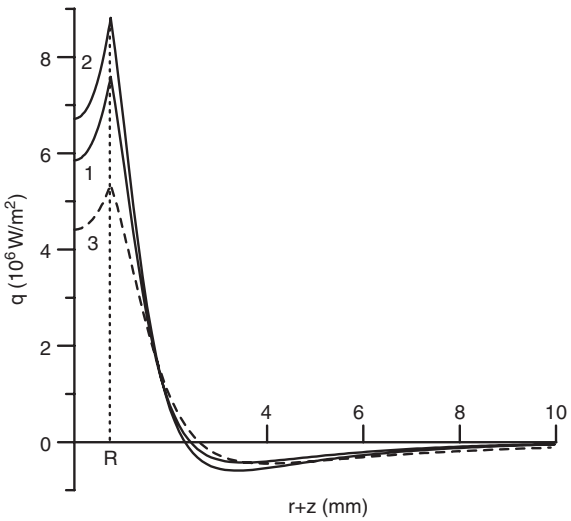

Figure 16. Distribution of the energy flux density along the surface of a tungsten cathode. $R = 0.75$ mm. 1: $I = 2$ A, $h = 19$ mm; 2: $I = 6$ A, $h = 19$ mm; 3: $I = 2$ A, $h = 29$ mm.

considered, and decreases with an increase of h (at $I = 2$ A, it is equal to 29 K for $h = 19$ mm and to 21 K for $h = 29$ mm). With an increase of current, the surface temperature increases. The temperature distributions along the front surface of the cathode for different cathode heights and the same current are very close but the temperature is a little higher in the case of a shorter cathode. Note that the latter occurs only if the lateral surface of the cathode is current collecting; the effect is reverse if the lateral surface is insulating.

The electron temperature distribution along the cathode surface is also non-monotonic, which is a consequence of the above-mentioned non-monotony of T_w. Values of the electron temperature are relatively low, which indicates that all points of the cathode surface operate on the growing section of the dependence of q on T_w under the conditions considered. This conforms to the above-mentioned fact that the modelling results for the conditions considered are not appreciably affected by the modifications introduced in this work into the model [22]. T_e on the front surface decreases with an increase of h, which is a consequence of the fact that the near-cathode voltage drop decreases with an increase of the cathode height at a fixed current, and also of the above-mentioned small decrease of the temperature of the front surface of the cathode with an increase of h.

Distribution of the electric current density (figure 15) is also similar to the distribution of the surface temperature, except that the current density, being (at U fixed) a strong function of T_w, shows a more noticeable variation along the front surface of the cathode and decreases much faster along the lateral surface. It is interesting to note that the total area of the current-collecting surface of the cathode is essentially the same for all the three variants.

Distribution of the density of the energy flux (figure 16) is quantitatively similar to the distribution of the electric current density, except that the energy flux density turns negative at $z \gtrsim 2$ mm.

6. Concluding remarks

Three modifications have been introduced in this work into the model of the near-cathode plasma layer developed in [22]: the formula for the ion energy flux density has been changed, which amounts to introducing equation (10) as an expression for the density of the plasma-related energy flux to the cathode surface; the account of possible presence of multiply charged ions has been excluded since a contribution of these ions to the total ion current to the cathode surface is minor; a description has been changed of a dependence of the ion flux to the cathode surface on the ratio α of the ionization length to the mean free path for collisions of ions with neutral atoms. The effect produced by the first and third modifications is not substantial. The effect of absence of multiply charged ions is essential at moderate or high U and high T_w and results in a decrease of the energy flux by a factor of up to approximately 2.

Equation (10) represents a particular form of equation of conservation of energy in the near-cathode layer. Obviously, this equation must hold, in an appropriate form, for any model of the near-cathode layer. Some or other variants of the integral form of this equation, equation (13), are well known to experimentalists and have served as a basis for many attempts to deduce the near-cathode voltage drop from calorimetric measurements. Unfortunately, for most theoretical models of the near-cathode layer, a question of compliance with the equation of conservation of energy has not been considered and this equation seems not to be satisfied. It is unclear what consequences such an inconsistence may cause for some or other particular model.

Three different mechanisms have been found which can cause non-monotony of the dependence of q_p on T_w: overcoming of the increase of combined ion and plasma electron heating by an increase of thermionic cooling which occurs when the plasma approaches full ionization; non-monotony of the dependence of the ion current on the electron temperature which is caused by a deviation of the ion current from the diffusion value; rapid increase of the plasma electron heating which is subsequently overcome by thermionic cooling. These mechanisms are responsible, respectively, for the maximum of the dependence of q_p on T_w at low voltages and for the first and second maxima at high voltages.

A closed description of the plasma–cathode interaction has been obtained by numerically solving the nonlinear boundary-value problem for the temperature distribution inside the cathode body. In this paper, calculation results are given on the diffuse discharge under conditions of the Bochum model arc lamp. Powers removed by thermal conduction to the cooling fluid and irradiated from the surface, the cathode surface temperature and the near-cathode voltage drop are calculated as functions of the arc current and are in a good agreement with experimental data. It is found, in particular, that fraction of power transported by electrons to the bulk plasma as compared to the total power supplied to the near-cathode plasma layer varies and may be quite considerable, which obviously hinders determination of the near-cathode voltage drop from calorimetric measurements. Integral characteristics of the cathode are not strongly affected by a distribution of current and power over the top of the cathode under the conditions considered.

Results of numerical modelling of the diffuse mode at high currents and of spot modes will be reported in the second part of the work.

Acknowledgments

The work was performed within activities of the project *Theory and modelling of plasma–cathode interaction in high-pressure arc discharges* of the program POCTI of Fundação para a Ciência e a Tecnologia and FEDER, of the project *NumeLiTe* of the 5th Framework programme ENERGIE of the EC and of the action 529 of the programme COST of the EC.

References

[1] Jüttner B 2001 *J. Phys. D: Appl. Phys.* **34** R103–23
[2] Bade W L and Yos J M 1963 Theoretical and experimental investigation of arc plasma-generation technology: Part II, vol 1. A theoretical and experimental study of thermionic arc cathodes *Technical Report* No ASD-TDR-62-729, Avco Corporation, MA USA
[3] Neumann W 1987 *The Mechanism of the Thermoemitting Arc Cathode* (Berlin: Akademie-Verlag)
[4] Hantzsche E 1992 *Contrib. Plasma Phys.* **32** 109–69
[5] Beilis I 1995 *Handbook of Vacuum Arc Science and Technology: Fundamentals and Applications* ed R L Boxman, D M Sanders and P J Martin (Park Ridge, NJ: Noyes Publications) pp 208–56
[6] Moizhes B Y and Nemchinskii V A 1974 *Sov. Phys. Tech. Phys.* **18** 1460–4
[7] Nemchinskii V A 1979 *Sov. Phys. Tech. Phys.* **24** 764–71
[8] Moizhes B Y and Nemchinskii V A 1975 *Sov. Phys. Tech. Phys.* **20** 757–62
[9] Benilov M S 1993 *Phys. Rev.* E **48** 506–15
[10] Benilov M S 1994 *IEEE Trans. Plasma Sci.* **22** 73–7
[11] Benilov M S 1998 *Phys. Scr.* **58** 383–6
[12] Benilov M S 1998 *Phys. Rev.* E **58** 6480–94
[13] Bötticher R and Bötticher W 2000 *J. Phys. D: Appl. Phys.* **33** 367–74
[14] Coulombe S 2000 *53rd Gaseous Electronics Conf.* (*Bull. Am. Phys. Soc.* **45** 18)
[15] Krücken T 2001 *Proc. 9th International Symp. on the Science and Technology of Light Sources (Cornell University, Ithaca, August 2001)* ed R S Bergman (Ithaca, NY: Cornell University Press) pp 267–8
[16] Bötticher R and Bötticher W 2001 *J. Phys. D: Appl. Phys.* **34** 1110–15
[17] Graser W 2001 *Proc. 9th International Symp. on the Science and Technology of Light Sources (Cornell University, Ithaca, August 2001)* ed R S Bergman (Ithaca, NY: Cornell University Press) pp 211–12
[18] Bötticher R and Bötticher W 2001 *Proc. 9th International Symp. on the Science and Technology of Light Sources (Cornell University, Ithaca, August 2001)* ed R S Bergman (Ithaca, NY: Cornell University Press) pp 207–8
[19] Haken H 1978 *Synergetics, An Introduction* volume 1 of *Springer Series in Synergetics* (Berlin: Springer)
[20] Beilis I I 2001 *IEEE Trans. Plasma Sci.* **29** 657–70
[21] Ecker G 1973 *Z. Naturforsch.* **28a** 417–28
[22] Benilov M S and Marotta A 1995 *J. Phys. D: Appl. Phys.* **28** 1869–82
[23] Luhmann J, Nandelstädt D, Barzik A and Mentel J 1999 *Proc., Contributed Papers, XXIV International Conf. on Phenomena in Ionized Gases (Warsaw, 1999)* ed P Pisarczyk, T Pisarczyk and J Wolowski, vol 1 (Warsaw: Institute of Plasma Physics and Laser Microfusion) pp 13–14
[24] Mentel J, Luhmann J and Nandelstädt D 2000 *Proc. 2000th IEEE Conf. on Industry Applications (Rome, October 2000) (Piscataway, NJ: IEEE)*
[25] Mentel J, Dabringhausen L, Lichtenberg S, Luhmann J, Nandelstädt D and Redwitz M 2001 *Proc. 9th International Symp. on the Science and Technology of Light Sources (Cornell University, Ithaca, August 2001)* ed R S Bergman (Ithaca, NY: Cornell University Press) pp 177–88
[26] Dabringhausen L, Nandelstädt D, Luhmann J and Mentel J 2002 *J. Phys. D: Appl. Phys.* **35** 1621–30
[27] Luhmann J, Lichtenberg S, Langenscheidt O, Mentel J and Benilov M S 2002 *J. Phys. D: Appl. Phys.* **35** 1631–8
[28] Nandelstädt D, Redwitz M, Dabringhausen L, Luhmann J, Lichtenberg S and Mentel J 2002 *J. Phys. D: Appl. Phys.* **35** 1639–47
[29] Hu W, Dawson F P and Benilov M S 1998 *Proc. 8th International Symp. on the Science and Technology of Light Sources (Greifswald, Germany, September 1998)* ed G Babucke (Greifswald: Institute for Low-Temperature Plasma Physics) pp 306–7
[30] Wendelstorf J 1999 *Proc., Contributed Papers, XXIV International Conf. on Phenomena in Ionized Gases (Warsaw, 1999)* ed P Pisarczyk, T Pisarczyk and

J Wolowski, vol 2 (Warsaw: Institute of Plasma Physics and Laser Microfusion) pp 227–8
[31] Nielsen T, Kaddani A and Benilov M S 2001 *J. Phys. D: Appl. Phys.* **34** 2016–21
[32] Fischer E 1987 *Philips J. Res.* **42** 58–85
[33] Flesch P and Neiger M 1998 *Proc. 8th International Symp. on the Science and Technology of Light Sources (Greifswald, Germany, September 1998)* ed G Babucke (Greifswald: Institute for Low-Temperature Plasma Physics) pp 406–7
[34] Flesch P and Neiger M 1999 *IEEE Trans. Plasma Sci.* **27** 18–19
[35] Flesch P and Neiger M 2001 *Proc. 9th International Symp. on the Science and Technology of Light Sources (Cornell University, Ithaca, August 2001)* ed R S Bergman (Ithaca, NY: Cornell University Press) pp 307–8
[36] Almeida R M S, Benilov M S and Naidis G V 2000 *J. Phys. D: Appl. Phys.* **33** 960–7
[37] Benilov M S 1995 *J. Phys. D: Appl. Phys.* **28** 286–94
[38] Benilov M S and Naidis G V 1998 *Phys. Rev.* E **57** 2230–41
[39] Voronov G S 1997 *Atomic Data and Nuclear Data Tables* **65** 1–35
[40] Devoto R S 1973 *Phys. Fluids* **16** 616–23
[41] Murphy E L and Good R H 1956 *Phys. Rev.* **102** 1464–73
[42] Benilov M S 1999 *J. Phys. D: Appl. Phys.* **32** 257–62
[43] Menart J, Heberlein J and Pfender E 1999 *J. Phys. D: Appl. Phys.* **32** 55–63
[44] Press W H, Teukolsky S A, Vetterling W T and Flannery B P 1992 *Numerical Recipes in FORTRAN* 2nd end (Cambridge: Cambridge University Press)
[45] Touloukian Y S, Powell R W, Ho C Y and Clemens P G 1970 *Thermal Conductivity. Metallic Elements and Alloys (Thermophysical Properties of Matter vol 1)* (New York–Washington: IFI/Plenum)
[46] Morrow R and Lowke J J 1993 *J. Phys. D: Appl. Phys.* **26** 634–42
[47] Nandelstädt D, Luhmann J, Micheldt B and Mentel J 1998 Private communication